innoTRAC Journal
Volume 3 (2024), pp. 76–92
https://doi.org/10.14464/innotrac.v3i1.772

Some aspects of modelling the coupled thermo-elasto-plastic behavior of a coating-rope-pulley system for bending fatigue analysis

Ivan Pechenizkiy[1*], Martin Anders[1], Thorsten Schmidt[1]

[1] *Chair of Material Handling, Dresden University of Technology, Dresden, 01069, Germany*

* *Correspondence: ivan.pechenizkiy@tu-dresden.de; Tel.: +49-3514-6334-222*

Peer reviewed article
Received 12 August 2024; Revised 02 Sept 2024; Accepted 03 September 2024; Available online December 2024

ABSTRACT Conducting a reduced multiple factor experiment, bringing a coating–rope–pulley system to a critical state due to cyclic bending and creating a family of predictive S-N curves requires, among other things, availability of reliable, quickly implemented mechanisms for intermediate control and accounting of special features of the mechanics and tribology of a process at the meso level. The implementation of this kind of mechanisms is possible on the basis of coupled FEA.

The paper discusses some aspects of modeling the coupled thermo-elasto-plastic behavior of coating and rope materials, contacting as a system with a rotating pulley. A distinctive feature of mentioned process is the presence of a technical contradiction, which consists in the fact that, under certain initial and boundary conditions, a coating provides a more favorable composition of a stress-strain state (SSS), resulting in an increase in the number of bending cycles. On the other hand, a coating heat insulator material may begin also to intensively interfere with convective removal of heat, generated in an elasto-plastically deformable rope, which entails a change in the dynamics of contact, the properties of coating material and a deterioration in the overall picture of SSS. This may result in a reduction in the number of endurable cycles. Thus, the creation of a FE-tribo-mechanical model is focused not only on obtaining a predictive tool for estimating the lifetime, but also on finding technically advantageous conditions for testing or operation.As a mechanism for a verification of the FE-model, it is suggested to use experimental diagrams of normal and tangential force distribution along the groove of a pulley, diagrams of thinning of a coating wall, azimuthal inhomogeneity of a rope external diameter and a thermal response of a system.

KEYWORDS Coated wire ropes, Thermo-mechanical analysis, Fatigue, Stress-Strain State, Finite Element Method, Archimedes-Screw-like transformation, Ansys Parametric Design Language, Nodes coupling, Volumetric heat source, Taylor-Quinney coefficient.

1. Introduction

A series of independent exploratory experiments, aimed at establishing the nature of the influence of polymer coatings of steel wire ropes on the critical number of cycles of their alternating bending loading, conducted at the Chair of Material Handling (CMH), Dresden University of Technology [1, 2], revealed the presence of significant potential for modifications of some rope designs, expressed in the growth of the service life of tested products under certain conditions by up to 30 % and more. Such a positive effect of polymer coatings can be explained from the standpoint of solid mechanics by the creation of a more favorable scheme of a Stress-Strain State (SSS) in a zone of maximum stress intensities due to a decrease in stress amplitudes, caused by the spread of the loads. Besides this, the mentioned effect can also be caused by an increase in the efficiency of the product redundancy, associated with the occurrence of an additional limitation on the ability of a damaged steel wire to leave its working position while partially retaining its functionality. Further to this, polymer coatings insulate a rope body from some external chemically aggressive media, fine abrasive and non-abrasive particles, occasional moderate mechanical damage, caused by external macrobodies and create a closed mechanical system that prevents an escape of mineral, synthetic or organic oils from a zone of heavy loading.

To be able to quickly establish more precise boundaries for the service life of variable polymer-coated rope designs, CMH is simultaneously developing several S-N predictive analytical models of varying degrees of complexity, one of the organizational elements of which is an accurate consideration of the temperature-dependent mechanical properties of polymers.

It is known from the theory and practice of mechanical and nuclear engineering that deformation of materials is accompanied by the transformation of mechanical work into other types of energy – thermal [3, 11], electromagnetic [11, 12], acoustic [11], etc. It is also known that cyclic alternating mechanical loads in some cases can lead to significant heating of deformable elements. Since steel wire ropes during fatigue tests are subjected to local plastic deformations leading to heat release, and (mostly) convective heat removal in the presence of polymer shell is hampered due to the low thermal conductivity of a coating, an undesirable thermal creep scenario may be initiated, in which, due to possible irrational choice of the loading rate either on a test rig or under real operating conditions, a polymer layer, due to excessive heating and intense mechanical loading, may break its integrity long before the steel core breaks.

In this regard, within the framework of the mechanism of intermediate control and consideration of special features of the mechanics and tribology of the process at the meso level being developed, there is a need for an adapted methodology for analytical assessment of the thermal state of the coating – rope – pulley system at an acceptable organizational and engineering-technical level.

2. Methods

2.1. Problem Statement

A pulley of radius R_0, brought into a state of alternating rotation with an angular velocity ω_0 at an angle of $\pm\phi_0$ on a test rig for parallel evaluation of the critical number of cycles N of alternating bending loading, leads to the passing of a rope (Pos. 4) through a three-element system of steel pulleys of radius R and thickness δ (Pos. 3), loaded through a hydraulic cylinder (Pos. 1) and auxiliary elements (Pos. 2, 5) with a force F. Here, the rope category is RCN 23-3, the area of metalized cross-section is A, the metallization material is structural steel, the rope coating material is extruded commercial polymer, the coating thickness is δ_{CT}, the outer diameter of the uncoated rope is d, the linear dimensions of the system are L_1-L_{10}) [Figure 1, Table 1]. As a result of such loading, the polymer coating of the rope is subjected at various stages, among other things, to the effect of thermal creep, which cannot be ignored at certain angular velocities. To analytically describe this effect and extend its results to a wide range of products and operating / testing conditions, it is necessary to obtain a consistent model and experimentally confirmed understanding of the dynamics of the temperature field in the active loading zone.

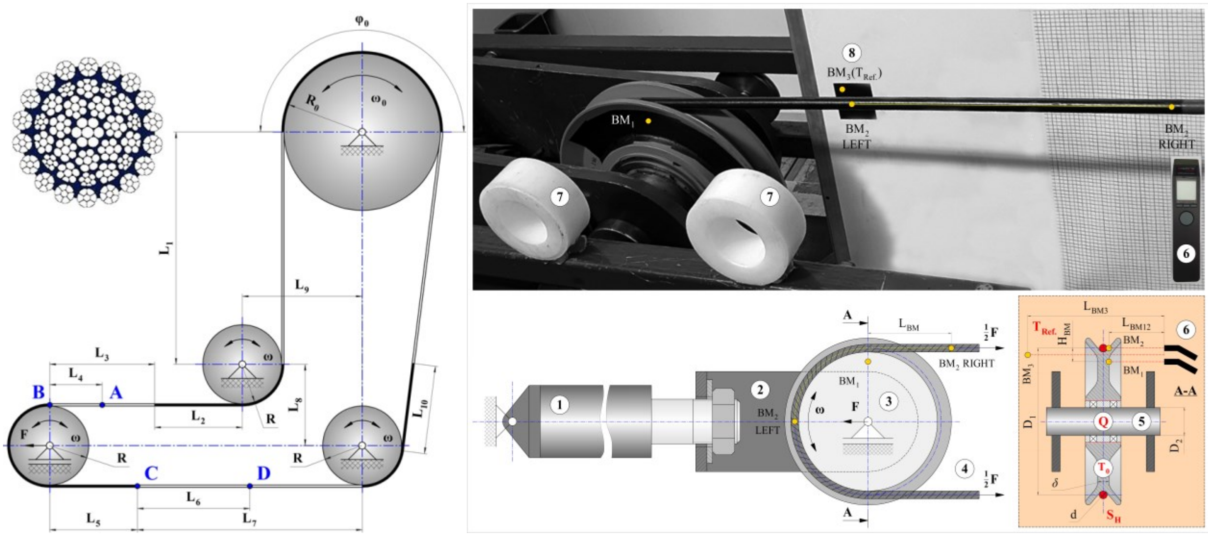

Figure 1: Scheme of the test rig and its local section, equipped for conducting an express exploratory experiment to determine the nature of thermophysical processes occurring in the rope in section A-B-C-D (Benchmark $BM_{2\ LEFT}$ - $BM_{2\ RIGHT}$), in the pulley (Benchmark BM_1) and in the adjacent environment (Benchmark BM_3): 1 - hydraulic cylinder, providing permanence of the force F throughout the experiment; 2 - auxiliary equipment, ensuring the required spatial position and degrees of freedom of the pulley; 3 - pulley with bearings and a darkened area for temperature measurements (Benchmark BM_1); 4 - tested rope with a darkened area for temperature measurements (Benchmark $BM_{2\ LEFT}$ - $BM_{2\ RIGHT}$); 5 - shaft; 6 - mobile non-contact pyrometer "Optris® MS"; 7 – auxiliary equipment for operational positioning of the pyrometer (H_{BM} = 0,02 m, L_{BM12} = 0,18 m, L_{BM3} = 0,35 m, L_{BML} = 0,14 m); 8 – platform with a coordinate grid of 0,005 x 0,005 m and a darkened place for measuring the ambient temperature $T_{Ref.}$ (Benchmark BM_3).

It should be noted that the solution of non-reduced nonlinear contact multi-object problems of one- and two-way coupled thermodynamic analysis is a resource-intensive process. At the same time, the procedures for reducing the dimensionality of problems and reducing the computational time interval, which are often used under conditions of limited computational capacities, lead either to a systematic distortion of the results of a numerical experiment or to the loss of the relevant part of the data associated with a reduced metric. In this regard, a rational choice of the computational scheme and extrapolation approaches is a serious source of resource savings and an important factor influencing the degree of subsequent scaling of the obtained results.

In the problem under consideration, in connection with the indicated difficulties, it is proposed to use a special physical and topological transformation of space, which makes it possible, at least at this stage, to replace the mechanical movement and deformation of the coating – rope – pulley system with the coordinated movement of the thermal load along static transformed objects. Such kind of transformation will allow to reduce the number of equations solved in one iteration by excluding the mechanical component from the system and related information transfer procedures. At the same time, obtaining an analytical representation of the dynamics of the temperature field in the active loading zone still seems possible and verifiable by the results of a field experiment without any additional transformations.

Table 1: Geometric and mechanical parameters of the test rig system.

Parameter	Unit	Value
Force F	[N]	35200
Angular velocity ω_0	[s^{-1}]	0,935
Area of metallization A	[m^2]	8,143 x 10^{-5}
Angle of rotation ϕ_0	[rad]	$\pm\pi$
Radius R_0	[m]	0,55
Radius R	[m]	0,126
Diameter D_1	[m]	0,266
Diameter D_2	[m]	0,05
Diameter d	[m]	0,012
Thickness δ	[m]	0,014
Thickness δ_{CT}	[m]	0,001
Length L_{BM12}	[m]	0,18
Length L_{BM3}	[m]	0,35
Length L_1	[m]	3,68
Length L_2	[m]	1,541
Length L_3	[m]	0,979
Length L_4	[m]	0,4895
Length L_5	[m]	1,052
Length L_6	[m]	1,084
Length L_7	[m]	2,168
Length L_8	[m]	0,4
Length L_9	[m]	0,7
Length L_{10}	[m]	1,052

2.2. Plan of numerical experiment

1. Work, spent on the plastic deformation:

The energy balance of plastic deformation could be determined by the equality of the work of strain $A\varepsilon$ (1) to the sum of the released heat Q and latent (stored due to generation, motion, blocking, and annihilation of microstructure defects) energy E_L [6]. One can describe the contribution of these components to the work, spent on the deformation, by the Taylor-Quinney coefficient $\beta = Q / A\varepsilon$ [3]. It was shown in [4, 5] that β can acquire for steels the values from 8-14-20 % to even 60-80 %, depending on alloy type, preliminary heat treatment of specimens, their stresses and strains, strain rates, SSS.

$$A_\varepsilon = \int_{\varepsilon-el.}^{\varepsilon-pl.} \sigma \, d\varepsilon. \tag{1}$$

Where:

$A\varepsilon$	- work of strain (ε-el., ε-pl.),	[J]
ε-el., ε-pl.	- elastic and plastic strain resp.,	[-]
σ	- stress,	[Pa]

2. Heat generation rate:

A numerical solution of the differential equation (2) with three classical types of boundary conditions (temperature acting on a surface; heat flux acting on a surface; convection on a surface), where the heat generation rate is represented by the fraction of plastic work converted into heat $\ddot{q} = \beta A\varepsilon$ and the boundary conditions describe a specific state of the simulated section of the test rig and the rope at a given moment in time, allows us to determine the dynamic temperature field in the local area of interest:

$$\rho C\left(\frac{\partial T}{\partial t} + V_X\frac{\partial T}{\partial x} + V_Y\frac{\partial T}{\partial y} + V_Z\frac{\partial T}{\partial z}\right) = \ddot{q} + \frac{\partial}{\partial x}\left(K_X\frac{\partial T}{\partial x}\right) + \frac{\partial}{\partial y}\left(K_Y\frac{\partial T}{\partial y}\right) + \frac{\partial}{\partial z}\left(K_Z\frac{\partial T}{\partial z}\right). \tag{2}$$

Where:

ρ	- density,	[kg/m^3]
C	- specific heat,	[J/kg-C]
T	- temperature,	[C]
$V_{X,Y,Z}$	- velocity vector for mass transport of heat,	[m/s]
$\ddot{q}$	- heat generation rate per unit volume,	[W/m^3]
$K_{X,Y,Z}$	- conductivity in x, y, z directions resp.,	[W/m-C]

3. Extrapolation of the solution results:

Using, in turn, the well-known empirical Newton's law of cooling (3-4) for extrapolating the obtained solution of the equation (2) to a larger time interval for each zone of interest, provided that the temperature regime in this zone is in a certain point of time of acceptable temporal and spatial homogeneity, thus allows us to further rationalize the methodology and to reduce the total calculation time:

$$\frac{\partial \mathrm{T}}{\partial \mathrm{t}} = \mathrm{s}(\mathrm{T}_{\mathrm{Ref.}} - \mathrm{T}); \tag{3}$$

$$\mathrm{T}(\mathrm{t}) = \mathrm{T}_{\mathrm{Ref.}} + \mathrm{e}^{-\mathrm{st}}(\mathrm{T}_0 - \mathrm{T}_{\mathrm{Ref.}}). \tag{4}$$

Where:

s	- empirical coefficient,	[s^{-1}]
$T_{Ref.}$	- reference temperature,	[C]
T_0	- initial temperature,	[C]

4. Numerical method of solution, Hard- and Software demands:

It is convenient to solve the equations (1, 2) in an integrated CAD-CAE platform Ansys 2023 R2 Mechanical Enterprise on low-demanding Hardware (e.g., Intel(R) Core i5-8250U / CPU@1,6 GHz / 64-Bit-OS / 2GB RAM) using the Finite Element Method FEM. Extrapolation of the results (4), in turn, does not have any special requirements for Soft- and Hardware.

5. Verification method:

Verification of the solution steps (1-2-3) can be implemented by comparing simulated temperature fields with the real temperature fields, determined on an experimental quickly reconfigurable test rig, the scheme and operating principle of which are shown above [Figure 1, Table 1].

6. Thermal creep (next stage of a numerical experiment):

The effect of thermal creep can be considered by solving a general mechanical problem, taking into account the temperature fields through the well-known and widely used Norton-Baily equation (5):

$$\varepsilon_{CREEP} = \mathrm{A}\sigma^n t^m e^{-\frac{Q}{RT}}. \tag{5}$$

Where:

ε_{CREEP}	- creep strain,	[-]
A	- material constant,	[consistent with σ, t, m, n]
σ	- stress,	[Pa]
t	- time,	[s]
T	- temperature,	[C]
Q	- activation energy,	[J/mol]
R	- Boltzmann's constant,	[J/C]
m, n	- material constants,	[-]

2.3. General assumptions

In the context of the problem being solved, we will assume that the Taylor-Quinney coefficient $\beta = 0{,}1 \neq f(t)$. The elementary section of the rope, subjected to the load $H_S = \ddot{q} = \beta A \varepsilon$, W/m^3 has homogeneous material and the thermal load H_S is distributed along it homogeneously at each moment of time according to [Figure 7] without oscillations inherent in the real process due to oscillations of the force F (±350 N). Two elementary sections loaded by H_S simultaneously and symbolizing the entry and the exit points of a rope have the same thermal load value. The load Q, W/m^2, describing the source of heat released due to friction in the bearings [Figure 1], is homogeneous in the azimuthal direction and is significantly less intense than the main heat source H_S. All thermal contacts of the problem are assumed to be ideal. The ambient temperature $T_{Ref.}$ is assumed to be constant. The increase in the linear dimensions of objects due to changes in their temperature is not taken into account. Of the significant geometric simplifications, it is worth noting the replacement of the circular cross-section of the rope (with a known metallization fraction of an area of a diameter d = 0,012 m) with a square solid cross-section (with a total area of $1{,}44\text{x}10^{-4}$ m^2) and the presence of several physical and topological transformations described below.

2.4. Physico-topological transformation

The topological transformation of the coating – rope – pulley system is realized through the coordinated rolling of the linear coating-rope elements into a helix in such a way that the inner diameter of the helix D corresponds to the outer diameter of the original pulley element D_1-d, the pitch of a helical turn S is equal to the doubled diameter of the original section of the coating element 2d and the length of the helix L is identical to the original length of the studied rope $L_{A\text{-}B\text{-}C\text{-}D}$ [Figure 1]. At the same time, to ensure the geometric-chronological continuity of the entire coating – rope – pulley contact zone, the original pulley is cut along the radial direction to the center and rolled into an Archimedes Screw in such a way that the number of full turns (3x360°) is guaranteed to cover the actual contact zone of the system (2x360°+36°) during one loading cycle [Figure 2].

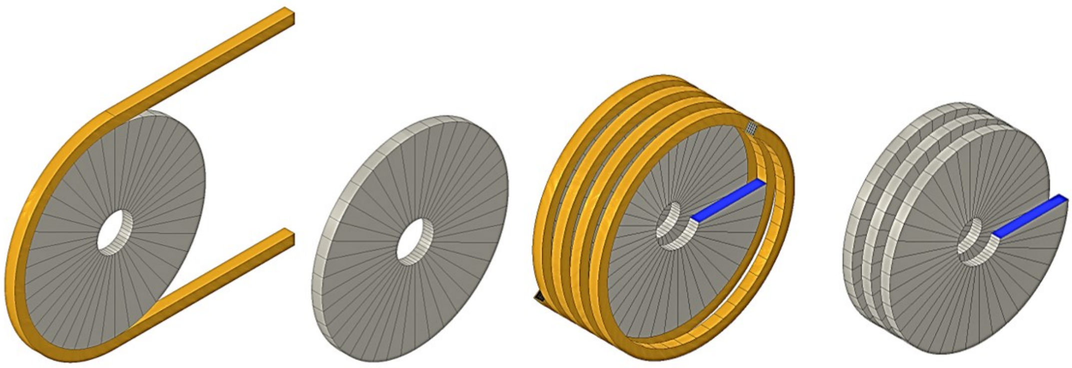

Figure 2: Idealized untransformed (left) and topologically transformed (right) systems.

The physical transformation of the coating – rope – pulley system is implemented through modification of the relevant thermophysical material parameters of the topologically transformed pulley, dependent on the volume (which is tripled in the case under consideration): thus, the density ρ_{TRANSF} = 1/3 $\rho_{UNTRANSF}$, kg/m^3; thermal conductivity K_{TRANSF} = 1/3 $K_{UNTRANSF}$, W/m-C. In addition, the condition of equality of temperatures T_{TRANSF} (t, r, ϕ) of all dependent points of the pulley space, having a different axial coordinate z, is additionally introduced (and implemented through a built-in User Defined Function UDF, written in Ansys Parametric Design Language APDL). The boundary condition of convective heat exchange, changed due to the increase in the azimuthal coordinate ϕ ($\Delta\phi_{max}$ = 0,06 %) and the associated changed area of the face-end surfaces of the pulley (ΔA = 0,2 %) do not participate in the thermophysical transformations at this stage due to low significance and are assumed to be unchanged. The coating and the rope do not participate in the physical transformation as well.

2.5. Validation of the physico-topological transformation

Let us suppose that the identity of the dynamic temperature fields of the transformed T_{TRANSF} (t, x, y, z) and untransformed $T_{UNTRANSF}$ (t, x, y, z) objects, arising during its symmetric loading with two identical local test heat flows Q = const = 3,6 MW/m^2, which are in its turn knowingly hyperbolized to highlight possible programming and understanding errors, is a criterion for the validity of the physico-topological transformation of the pulley computational space. One has to mention that a test heat flow Q here is a principal analogy of a heat flow, arising in a coating – pulley dynamic contact zone. The removal of supplied heat in transformed and untransformed test pulleys could be then realized, in accordance with field test conditions, by convection on 4 free surfaces (h = 10 W/m^2-C, $T_{Ref.}$ = 28 C). The space and time discretization of the transformed and untransformed computational spaces are identical. The loading time in both cases is chosen to be identical as well and comparable to the model loading time of the studied case.

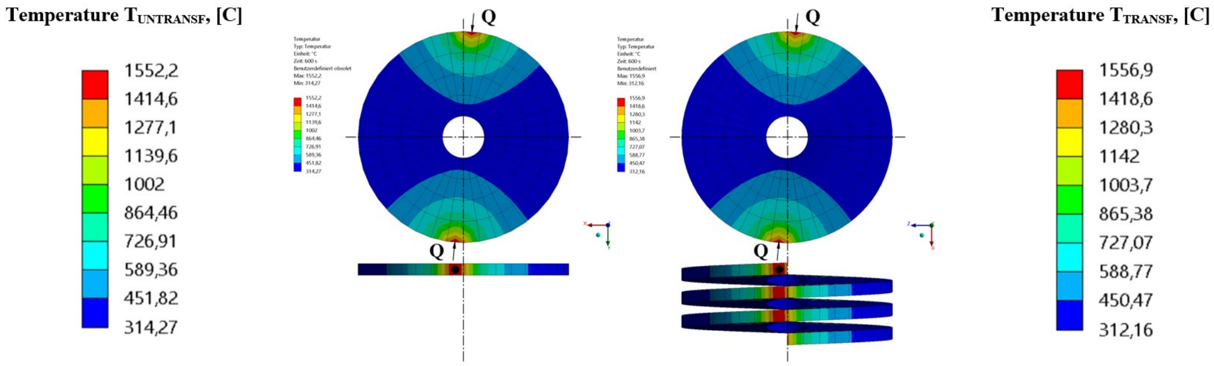

Figure 3: Loading scheme and temperature fields $T_{UNTRANSF}$ ($t=t_{END}$, x, y, z) and T_{TRANSF} ($t=t_{END}$, x, y, z) of untransformed (left) and physico-topologically transformed (right) objects.

The temperature field of the transformed object, localized at $t = t_{END}$ = 600 s in the zone of extreme values, has deviations from the temperature field of the untransformed object ΔT_{max} = + 0,3 %, ΔT_{min} = - 0,6 % with an acceptable repetition of the character of radial, azimuthal and axial gradients [Figure 3]. In addition to this, one can identify the desired artificial reproduction of the temperature field in associated finite elements in the direction of the vertical axis of transformed pulley. The achieved accuracy of repeatability of 2 numerical results within the framework of the numerical experiment validation is, as we suppose, satisfactory (ΔT, $\Delta(dT/dr)$, $\Delta(dT/d\phi)$, $\Delta(dT/dz)$ << 10 %).

Consequently, one can assess, at least at this stage, the applied concept of physico-topological transformation, as a valid one and use it further in solving similar problems.

2.6. Calculation of the load, generated by a volumetric heat source

To define a value of a thermal load S_H, W/m^3 [Figure 1], generated by a single volumetric heat source [Figure 4], let us solve a problem of triaxial homogeneous elasto-plastic deformation of a specimen by orthogonally oriented pressures p_x, p_y, p_z and find 10 % of the work of plastic deformation. The dimensions of the specimen (a x b) are taken as a first approximation such that its cross-sectional area is 1/9 of the cross-sectional area of the simulated rope core and is 0,004 x 0,004 m and the length (c) corresponds to the length of an arc of a circle with a radius R = 0,133+0,007 m and an opening angle of 9° [7] – 0,022 m. The material is taken to be identical to the core material, the mechanical properties of which could be described e.g., by the bilinear hardening law (μ = 0,3, E = 200 GPa, σ_Y = 250 MPa, Π = 1,45 GPa [8]). The pressures p_x and p_y, due to the close analogy of the local SSS patterns arising during rope loading and, for example, during a single-pass drawing of a cylindrical part on a die with rounding radii, are taken to be p_z^- = – 0,5 F/A = – 216,177 MPa [Table 1], $p_x^+ = p_y^+ = 0{,}5\ p_z^-$ = 108,088 MPa [9]. The loading time of the specimen corresponds to the time it takes the rope to pass through a 9° of pulley arc and is 0,04 s, which is equivalent to one loading step of the main problem. Since, with the declared SSS scheme ($\sigma_x^+ = \sigma_y^+ = 0{,}5\ \sigma_z^-$), the zones of the sample located on the orthogonal planes of symmetry do not undergo warping, it is convenient to represent the model as a 1/8 part (a/2, b/2, c/2) with a corresponding description of the boundary conditions: U_X (YOZ) = U_Y (XOZ) = U_Z (XOY) = 0 m.

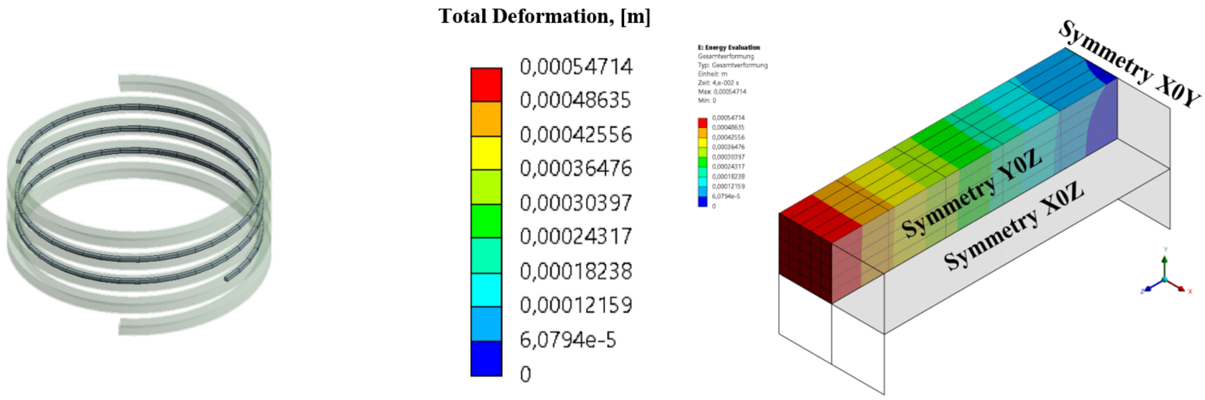

Figure 4: The procedure for evaluation of the thermal load S_H: the location of volumetric heat sources (left) and the calculation scheme of mechanical deformation of an elementary specimen with a field of the full vector of deformations at the final moment of loading time t = 0,04 s (right).

The total energy, calculated on the basis of the described conditions, including the kinetic E_{KIN}, thermoelastic E_{EL} and thermoplastic E_{PL} components, is E_{TOT} = 0,60043 J, from which, to separate the thermoplastic component, it is necessary to subtract E_{KIN} = 1,96 x 10^{-7} J and E_{EL} = 5,47 x 10^{-3} J. Taking into account the loading time (1/25 of a second), symmetry conditions (1/8 of the volume), the volume of the whole specimen (3,244 x 10^{-7} m^3) and the fraction of the energy, converted into heat (1/10), the value of the thermal load will be determined as: S_H = (0,60043 – 1,96 x 10^{-7} – 5,47 x 10^{-3}) x 25 x 8 x

1/3,244 x 10^{-7} x 0,1 = 36,68 MW/m^3. The stress and strain intensities, achieved under the described boundary conditions at the final moment of time are, respectively: σ_i = 324,08 MPa, ε_i = 0,0507.

It should be noted that a more accurate description of the dimensions of a deformation zone a x b x c, m, which generally are in a non-homogeneous elasto-plastic state, is a non-trivial, low-reducible, non-linear, multi-object, contact, coupled thermo-mechanical problem, the solution of which can also be obtained by the FEM method (one of the problems, being solving actually by CMH within the framework of modelling the coupled thermo-elasto-plastic behavior of a coating – rope – pulley system for bending fatigue). Additionally, we note that the linearized representation of the plastic zone itself in 3 directions, used in the solution at this stage, is not able (within the high accuracy requirements necessary for precise prediction of the number of fatigue test cycles) to correctly represent its actual geometry and must be described in some suitable discrete way.

Let us also note that the elements of a real rope experience some additional thermal load in the region of the highest and moderate normal stresses in the form of energy, generated by rubbing contact surfaces. This phenomenon can be accurately taken into account in calculations by using the Newton-Coulomb law with the corresponding energy dissipation coefficient. However, taking into account such a phenomenon requires some change in the calculation paradigm and in this problem is considered exclusively from the point of view of the potential for detailing future calculation scenarios.

2.7. Initial and boundary conditions, thermophysical properties of materials

For ease of interpretation, the initial and boundary conditions of the problem are presented below in the form of combined diagrams with accompanying information [Figure 5, 6, Table 2].

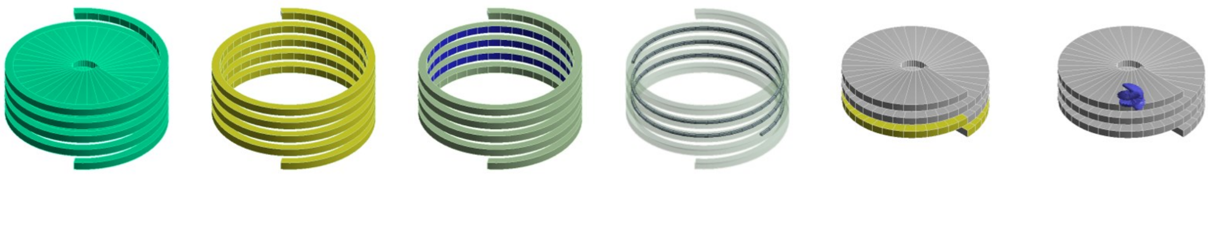

Figure 5: Initial and boundary conditions: a – initial temperature of bodies $T_{0\ COATING} = T_{0\ CORE} = T_{0\ PULLEY}$ = 27,1 C; b – surfaces of constant and potential (changing its type from convective to conductive at the moment of contact with the pulley) convective heat exchange of the coating, h = 10 W/m^2-C; c – evolving zone of ideal thermal contact, the status of which depends on the chronological step of loading [Figure 6]; d – evolving zone of location of volumetric heat sources S_H, W/m^3, the value of the magnitude and location of which depends on the chronological step of loading [Figure 6]; e – surfaces of constant and potential convective heat exchange of the pulley, subjected to physical and topological transformation [Chapter 2.4-2.5], h = 10 W/m^2-C; f – internal surfaces of the pulley, loaded with a heat flow, simulating the result of bearing influence and the value of which, in the first approximation, is preliminary assumed to be zero to enable subsequent separate assessment of the heat flow of minor importance, Q = 0 W/m^2. Due to the complexity of representing different-scale elements of the system design, the thermal insulation of the coating and the rope from both ends, simulating thermal planes of symmetry, is not

shown in the diagram, but is taken into account in the calculations as q = 0 W/m². The ambient temperature, based on experimental data, in the first approximation is taken to be averaged and constant over the entire time of simulation, $T_{Ref.}$ = 27,75 C.

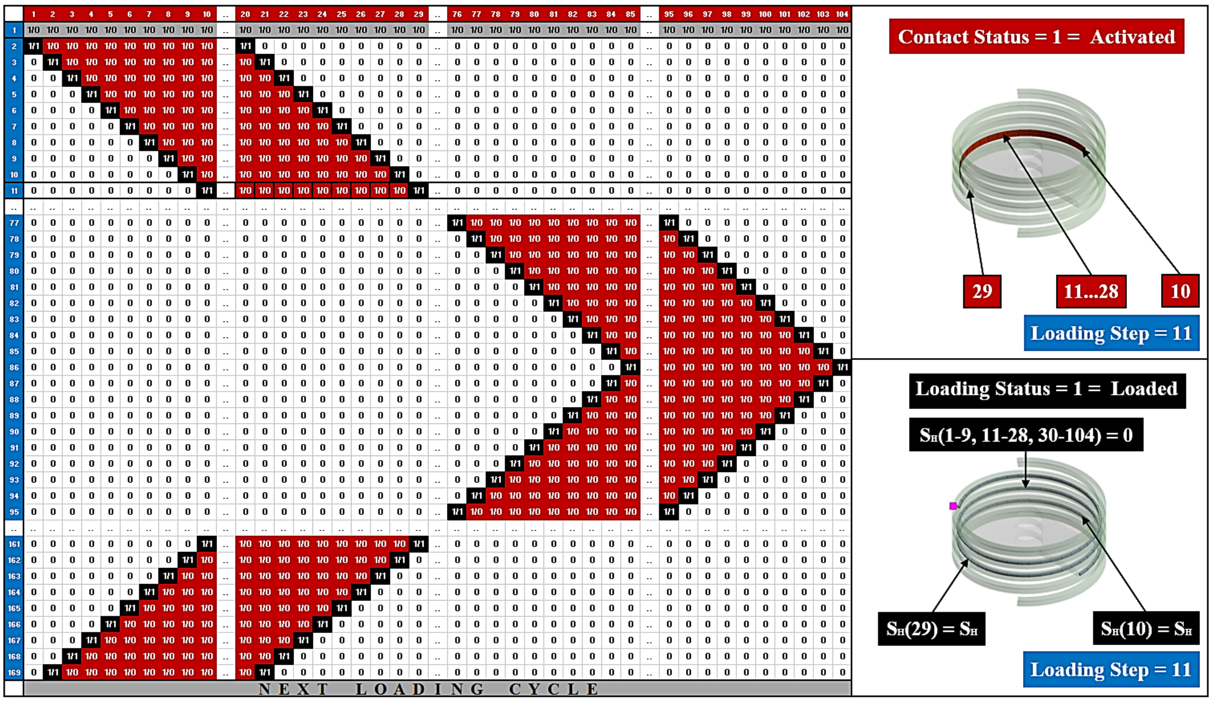

Figure 6: Scheme of volumetric heat source loading (S_H) and contact zone activation depending on chronological time step within one loading cycle: ■ – Time Step Number, Δt = 0,04 s; ■ – Contact Status of a contact pair (1 = activated, perfect thermal contact is active ($T_i = T_{i+1}$, C, $q_i = q_{i+1}$,W/m²); 0 = deactivated ($T_i \neq T_{i+1}$, C, $q_i \neq q_{i+1}$, W/m², forced convective heat exchange from both sides of deactivated contact with low speed flow of air over a surface is initialized instead (h = 10 W/m²-C)), corresponds to a nominator of a cell value); ■ – Loading Status (1 = loaded ($S_{Hi} = S_H$, W/m³); 0 = unloaded (S_{Hi} = 0 W/m³), corresponds to a denominator of a cell value); ■ – First Time Step of a single loading cycle. As an example, Time Step No. 11 and the corresponding statuses are shown: 10-29 – serial numbers of active contact pairs (in the model along the entire potentially active contact zone there are 104 contact pairs); 10, 29 – serial numbers of the rope core finite elements, which are affected by the thermal load S_H; the elements 1-9, 11-28 and 30-104 are in its turn not affected.

Table 2: Thermophysical properties of materials.

Density, ρ [kg/m³]		Th. Conductivity, K [W/m-C]		Specific heat, C [J/kg-C]	
Pulley:	2616,7	Pulley:	20,167	Pulley:	434
Rope core:	7850,0	Rope core:	60,500	Rope core:	434
Rope coating:	950,0	Rope coating:	0,280	Rope coating:	2300

3. Results

The result of the problem solution is the temperature T (x, y, z, t), calculated for each node of each finite element of the system on the time interval t E (0; t_{END}) with the time step Δt = 0,04 s. The temperature values of the Benchmarks $BM2_{LEFT}$ - $BM2_{RIGHT}$ [Figure 1]) $T_{BM2L, R}$ = f(t) are additionally extrapolated according to (3-4) on the time interval t E

(t_{END}; t_{STAT}) for the convenience of comparative analysis between the information obtained analytically and experimentally [Figure 8].

As an additional mechanism for monitoring the fundamental correctness of the solution, [Figure 7] shows the dynamic contact statuses of the "coating – pulley" pair, heat flow over the active contact zone and the temperature fields of the rope core in close proximity to the contact zone at the initial stage of heating, corresponding to identical moments of thermal loading of the system.

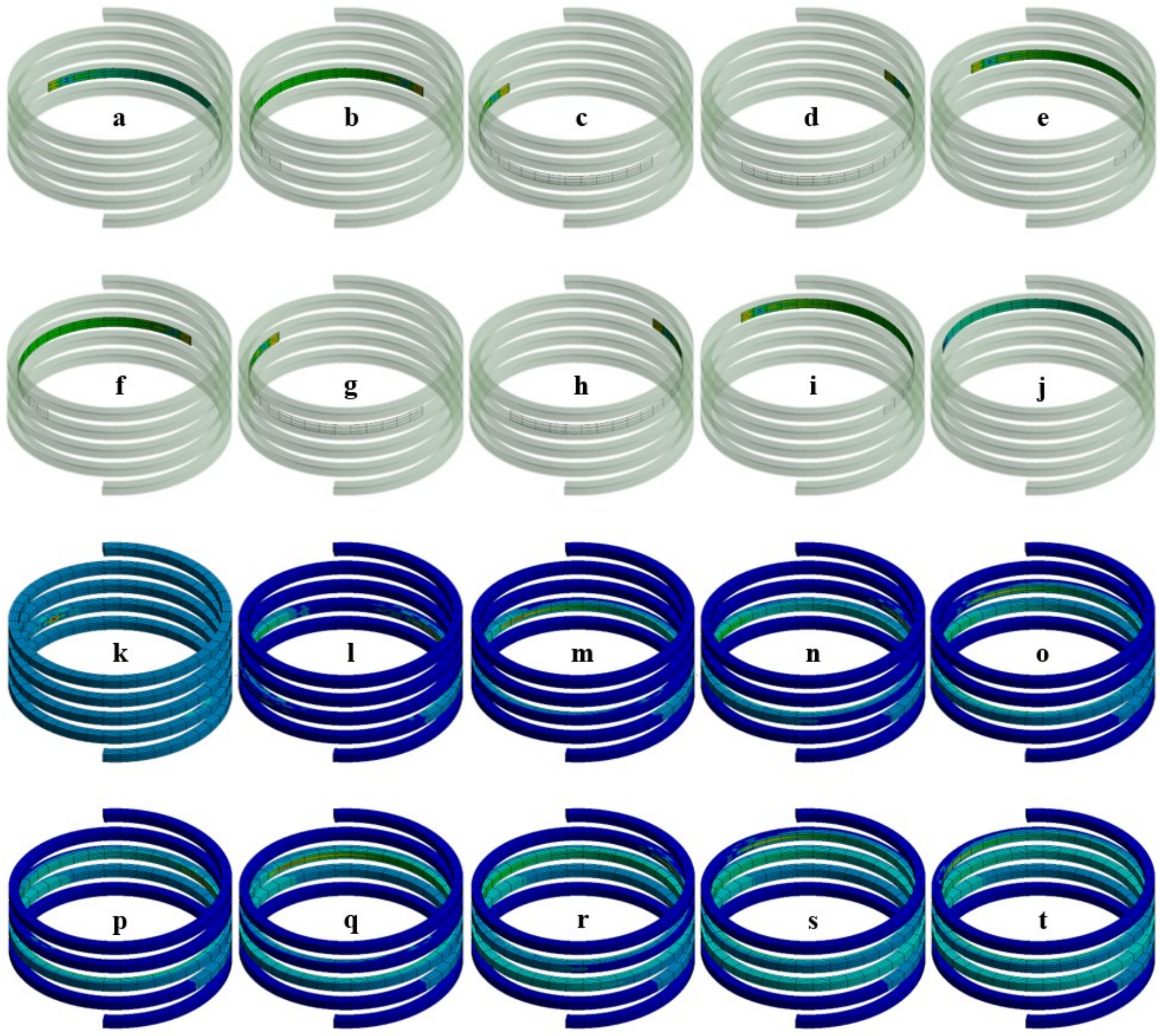

Figure 7: Evolution of the thermal contact zone and the heat flux q through the contact between the rope coating and the pulley (**a-j**) and the rope core temperature field T (x, y, z, t) (**k-t**) at times corresponding to 2, 12, 22, 32, 42, 52, 62, 72, 82 and 86 loading steps, discretely describing a half-cycle [Figure 6]. The scales for assessing the values of physical parameters are not shown due to their low significance in the time interval t E (0; 3,44 s), $\Delta T \approx 0{,}1\text{-}0{,}2$ C, $\Delta q \approx 50$ W/m^2.

It should be noted that the above-mentioned difficulty in solving multidisciplinary nonlinear contact problems without using expensive high-performance computational platforms, in this particular case resulted in the following values: number of elements – 4302, number of nodes – 22987, MAPDL Time – 12,75 h, MAPDL Volume – 69,706 GB.

In addition to the developed FE model, a simplified test rig with a related measuring procedure for express analysis of thermal fields of moving rope elements was designed, implemented and tested. It was found that the rig needed some thermo-physically relevant improvements, which one can by the upcoming more accurate series of measurements of combined thermo-mechanical fields formulate as follows.

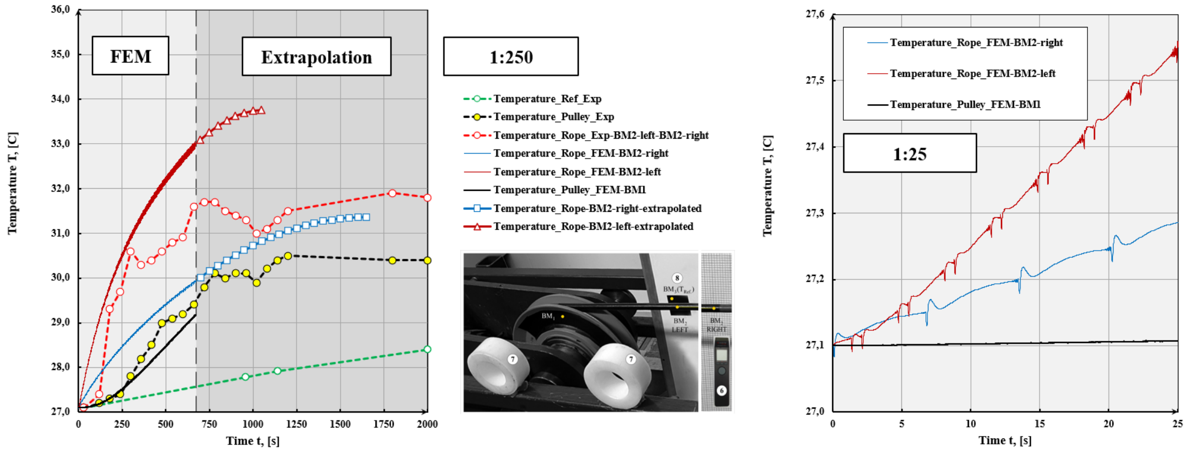

Figure 8: Temperature fields T = f(t) of the Benchmarks BM_1, $BM_{2\ LEFT}$ - $BM_{2\ RIGHT}$ and the ambient temperature $T_{Ref.}$, C: the fields are presented on the time interval t E (0; t_{END}) U t E (t_{END}; t_{STAT}), where for clarity and ease of analysis two time-axis scales are used: 1:250 (left) and 1:5 (right).

It is advisable to measure temperature fields and recalculated mechanical contact stresses of a rope with a signal sampling frequency of at least f_S = 10 Hz and a signal quantization depth, ensuring ΔT = 0,05 C and ΔF = 5-10 N on a single universal object of research. Since the dynamics of the process do not allow this type of measurement to be carried out directly on a rope, having in general case 4 degrees of freedom (DOFs) and supposed to have unique design characteristics, the measurements could be carried out indirectly through the engineering fitting of a pulley, having only 1 DOF, to a universal system of built-in autonomous sensitive elements, responsible to detect pressure change in the contact zone [7] and to describe its azimuthal distribution.

In turn, the temperature field on the pulley in the vicinity of the contact zone can be measured by means of contact measurement, for which the rotating outer-end surface must be prepared in the appropriate technical manner. The temperature field of the pulley must be measured at least at two points (circles) to be able simultaneously to characterize not only the body's response to an external load in the form of the above-mentioned H_S, but also the parasitic heat flux Q, caused by the operation of the bearing [Figure 1].

The measurement of temperature fields on a rope one can organize, as in the express experiment, in a contactless manner, which, however, will require the need for precise orientation of an autonomous pyrometer or a group of pyrometers due to an expectation of a significant temperature gradient along the cross-section caused by increased value of ω_0 [Chapter 2.1]. The analysis of the permissible phase shift of a signal, measured by different devices and the coordination of the flow of simultaneously incoming data was not performed at this stage.

Auxiliary equipment and positioning elements of the test rig must be compact, mobile and located on a single mounting platform.

The analysis of the requirements for the accuracy of the assessment of the thermophysical parameters of materials was not carried out in this work and is transferred to the next iteration of the research process.

4. Discussion

The analysis of the field experiment data [Figure 8] allows us to qualitatively characterize the obtained results as follows:

The experimental heating curves of the pulley and the rope have the form of a Verhulst curve (including the so-called accumulation and saturation zones), which agrees well with the typical heating curves of regular metal bodies, exposed to external heat flow under conditions of convective heat exchange with the environment. The experimental curves have a noticeable, but non-critical for this stage, spread of values, caused by the peculiarities of the conducted express experiment, which at subsequent stages of practical detailing of the thermodynamics of the process can be significantly leveled out by improving the measurement technique and a technical re-equipment. In addition, in the region of t E (750; 1000 s), an anomaly is observed that is repeated on both curves, which makes an assumption about the methodological error of the measuring process less likely (but does not exclude it completely) and allows us to assume with a greater degree of probability the presence of an influence of an unaccounted phenomenon. For example, a change in the friction mode inside the rope or bearing, an unrecorded local change in the temperature of the environment (the test site has a high irregular density of irregularly operating mechanical engineering equipment, which can be understood as additional heat sources), a radical local change in the heat exchange mode which is not associated with friction processes, a presence of an unaccounted external body of high thermal conductivity that has entered into a local thermal contact due to its linear thermal expansion, another unaccounted factor.

The field experiment curves can be quantitatively characterized as follows:

dT_{BM1}/dt = 0,0034 C/s, dT_{BM2}/dt = 0,0067 C/s, $T_{STAT\ BM1}$ = 30,5 C,

$T_{STAT\ BM2}$ = 31,9 C, $t_{STAT\ BM1}$ = 1750 s, $t_{STAT\ BM2}$ = 1750 s, ΔT_{STAT}= 1,4 C,

Δt_{STAT}= 0 s, Δ (dT/dt) = 197 %.

We have also to note that several single measurements of the ambient air temperature showed its inconstancy with a slight positive gradient.

The analysis of the numerical experiment data [Figure 8] allows us to qualitatively characterize the obtained results as follows:

The heating curve of the pulley has an accumulation zone that is practically identical to the accumulation zone in the field experiment, but cannot be extrapolated beyond the analyzed FEM zone (100 full loading cycles), since the condition for the possibility of extrapolation according to the law described in (3-4) is not met. To obtain the possibility of extrapolation, it is necessary to increase the period of simulated time during which the necessary mathematical conditions will be ensured. The simulated curves, describing the behavior of the Benchmark BM_2, have an extremely weakly expressed accumulation zone but can still be characterized by a Verhulst curve. We would like to emphasize that for demonstration and organizational purposes, the simulated coating material was chosen knowingly with reduced thermal conductivity, which, as expected, led to a slowdown in the cooling of the coating surface and insufficiently fast heating of the surface of the pulley, being in contact with it. When the coordinate grid is enlarged to (1:5), it can be seen that both curves have characteristic oscillations at the moment of heat flow transfer from the volumetric source. At the same time, at the very moment of the heat transfer, there is a drop in the curve, characterizing a thermal state of the rope, and a consistent rise in the curve, characterizing the heat-receiving pulley, to see. Due to the extremely small scale (even 1:5 is still insufficient), the pulley curve, which has a stepped shape, is still displayed on the graph on the right as a straight line, although it is not. The number of moments of heat transfer from the source to the receiver during one cycle lasting 6,8 s, corresponds to the number of events (moments of the rope point passing through the mechanical loading point) in the sequence (X – X – XX – X – X, where X – $BM_{2\,LEFT}$, XX – $BM_{2\,RIGHT}$ [Figure 8]) and is 5 events per cycle.

In addition, it should be noted that the simulated local topology of the temperature field is similar to temperature fields, observed when a volumetric heat source moves along a certain trajectory on a surface of small radius of curvature (e.g., when carrying out welding, cutting, recycling or some additive works by means of high energy methods [13]). As in the above-mentioned methods, during a relative motion of a source relative to a receiver, a drop-shaped thermal signature is observed with a shift of the energy extremum to the leading edge of the motion front [Figure 9].

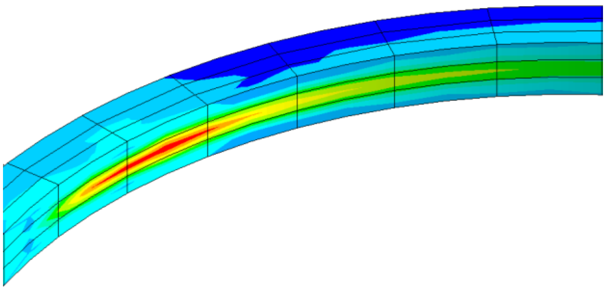

Figure 9: An element of a thermal signature of a single volumetric heat source, recorded at the time corresponding to [Figure 7m]. The direction of movement (counterclockwise) and a drop-like shape are clearly recognizable.

The numeric experiment curves can be quantitatively characterized as follows:

dT_{BM1}/dt = 0,0029 C/s, $dT_{BM2LEFT}/dt$ = 0,0087 C/s, $dT_{BM2RIGHT}/dt$ = 0,0041 C/s,

$T_{STAT\ BM2LEFT}$ = 33,8 C, $T_{STAT\ BM2RIGHT}$ = 31,3 C, $t_{STAT\ BM2LEFT}$ = 1050 s,

$t_{STAT\ BM2RIGHT}$ = 1650 s, Δ (dT_{LEFT}/dt) = 300 %, Δ (dT_{RIGHT}/dt) = 141 %.

Since the numeric experiment curves, describing the behavior of the Benchmark BM_2, form a space of function values in which the field experiment curve is located, and since the simulated curve, characterizing the pulley behavior, is almost identical to the field experiment on the simulated time interval, it can be assumed that the influence of the unaccounted parasitic heat flux Q is minor. Nevertheless, determining the value of the heat flux Q [Figure 1] is necessary to ensure the purity of the numerical experiment and the possibility of using the model for practical purposes with high accuracy requirements.

The potential capabilities of the developed FEM model can be characterized as follows:

The parameterized model is capable of limited variation of some process-relevant geometric parameters of the characteristic dimensions of a rope, a coating and a pulley, thermophysical properties of materials, values of thermal loading parameters and chronological characteristics of the process. As a result, it is possible to simulate thermal fields T (x, y, z, t) and their spatial and temporal gradients under various boundary conditions. In addition, the model serves as a source of data, describing the thermal state of a process, exported further to the thermo-mechanical problem to take into account the effect of thermo-creep of polymers (5) and thermo-mechanical stresses, caused by the linear expansion of materials.

In conclusion, we note that the thermal creep scenario arising under certain loading conditions must be strictly assessed mathematically. This is necessary to identify not only potentially dangerous combinations of process parameters, but also to find zones where thermal creep will have a neutral or even positive effect on the nature of the S-N curve family.

Acknowledgement

The authors would like to thank the Ministry for Economic Affairs and Climate Action of Germany BMWK for funding the research project «Dimension – Influence – Coated - Ropes». Our research team would also like to express its appreciation to our colleagues from Clausthal University of Technology / Chair of Machine Elements and Design (headed by Prof. Dr.-Ing. Armin Lohrengel), our cooperation partner – the company Trowis Gmbh and The European Federation of Steel Wire Rope Industries for the numerous recommendations, scientific-technical advice and support.

References

[1] T. Schmidt, A. Lohrengel, Lebensdauer und Wickelverhalten kunststoffummantelter Drahtseile, Schlussbericht zu IFG-Vorhaben 19598 BG, Technische Universität Dresden, Technische Universität Clausthal, S. 118, 2020.

[2] M. Schulze, A. Lohrengel, T. Recknagel, T. Schmidt, Lebensdauer und Wickelverhalten kunststoffummantelter Drahtseile, Tagungsband 26, Kranfachtagung, Dresden, S. 213, 2018.

[3] G. I. Taylor, H. Quinney, The Latent Energy Remaining in a Metal after Cold Working, Proceedings of the Royal Society A: Mathematical, Physical and Engineering Sciences, 143(849), pp. 307–326, 1934, doi:10.1098/rspa.1934.0004.

[4] B. A. Zimin, V. E. Sventitskaya, I. V. Smirnov, Y. V. Sudenkov, Influence of Strain Rate on Heat Release under Quasi-Static Stretching of Metals, Physics of the Solid State, Vol. 60, No. 4, pp. 758–763, 2018, doi:10.1134/S1063783418040352.

[5] P. Knysh, Y. P. Korkolis, Determination of the fraction of plastic work converted into heat in metals, Mechanics of Materials, V.86, pp. 71-80, 2015, doi:10.1016/j.mechmat.2015.03.006.

[6] S. P. Gadaj, W. K. Nowacki, E. A. Pieczyska, Investigation of temperature distribution during plastic deformation of stainless steel, QIRT 96, Eurotherm Series 50, Edizioni ETS, pp.4, 1997, doi:10.21611/qirt.1996.049.

[7] B. Häberle, Pressung zwischen Drahtseil und Seilscheibe, PhD-Thesis, Institut für Fördertechnik, Getriebetechnik und Baumaschinen der Universität Stuttgart, pp. 103, 1995.

[8] Ansys 2023 R2 Mechanical Enterprise Library of general linear and nonlinear materials, 2024.

[9] V. P. Romanovskiy, Handbook of Cold Stamping, Moscow, pp. 520, 1979 (Rus.)

[10] Z. Zhang, H. Yang, H. Li, N. Ren, Y. Tian, Bending behaviors of large diameter thin-walled CP-Ti tube in rotary draw bending, Progress in Natural Science: Materials International, V. 21, Issue 5, pp. 401-412, 2011, doi: 10.1016/S1002-0071(12)60076-8.

[11] O. P. Maksymkin, M. N. Husev, D. A. Toktohulova, Dissipative processes arising during plastic deformation of nickel and chromium-nickel alloys, irradiated with neutrons, Polzunovsky Almanac V. 1, pp. 110-114, 2007 (Rus.)

[12] R. Verreet, Magnetism in rope wires, Ingenieurbüro für Drahtseiltechnik Wire Rope Technologz Aachen GmbH, Aachen, S. 1-9, 2018.

[13] A. J. Ross, I. Bitharas, K. G. Perkins, A. J. Moore, Volumetric heat source calibration for laser powder bed fusion, Additive Manufacturing V. 60, pp. 1-14, 2022, doi: 10.1016/j.addma.2022.103267.